POLITECNICO DI TORINO
Repository ISTITUZIONALE

# Convergence acceleration aspects in the solution of the PN neutron transport eigenvalue problem

*Original*
Convergence acceleration aspects in the solution of the PN neutron transport eigenvalue problem / Abrate, Nicolo'; Ganapol, Barry D.; Dulla, Sandra; Saracco, Paolo; Ravetto, Piero; Zoia, Andrea. - ELETTRONICO. - (2021), pp. 1103-1112. (Intervento presentato al convegno Mathematics and Computation (M&C) 2021 tenutosi a Virtual Meeting nel October 3-7 2021).

*Availability:*
This version is available at: 11583/2970424 since: 2022-10-19T12:18:40Z

*Publisher:*
American Nuclear Society

*Published*
DOI:

*Terms of use:*

This article is made available under terms and conditions as specified in the corresponding bibliographic description in the repository

*Publisher copyright*
GENERICO -- per es. EPJ (European Physical Journal) : quando richiesto un rinvio generico specifico per

(Article begins on next page)

24 September 2024

# CONVERGENCE ACCELERATION ASPECTS IN THE SOLUTION OF $P_N$ NEUTRON TRANSPORT EIGENVALUE PROBLEM

**N. Abrate[1,*], B.D. Ganapol[2], S. Dulla[1,3], P. Saracco[4] , P. Ravetto[1,3] and A. Zoia[5]**

[1]Politecnico di Torino
Dipartimento Energia - NEMO Group
Corso Duca degli Abruzzi, 24 10129 - Torino (Italy)

[2]University of Arizona
Department of Aerospace and Mechanical Engineering
Tucson, AZ 85712, USA

[3]INFN - Sezione di Torino
Via Pietro Giuria, 1 10125 Torino (Italy)

[4]INFN - Sezione di Genova
Via Dodecaneso, 33 16146 - Genova (Italy)

[5]Université Paris-Saclay, CEA
Service d'études des réacteurs et de mathématiques appliquées (SERMA)
F-91191 Gif-sur-Yvette (France)

nicolo.abrate@polito.it, ganapol@cowboy.ame.arizona.edu, sandra.dulla@polito.it, paolo.saracco@ge.infn.it, piero.ravetto@polito.it, andrea.zoia@cea.fr

## ABSTRACT

The solution of the eigenvalue problem for neutron transport is of utmost importance in the field of reactor physics, and represents a challenging problem for numerical models. Different eigenvalue formulations can be identified, each with its own physical significance. The numerical solution of these problems by deterministic methods requires the introduction of approximations, such as the spherical harmonics expansion in $P_N$ models, leading to results that depend on the approximations introduced (spatial mesh size, $N$ order, ...). All these results represent, in principle, sequences that can easily profit from acceleration techniques to approach convergence towards the correct value. Such a reference value is estimated, in this work, by the Monte Carlo technique. The Wynn-$\varepsilon$ acceleration method is applied to the various sequences of eigenvalues emerging when tackling the solution of the $P_N$ models with different orders and increasing spatial accuracy, in order to obtain more accurate, benchmark-quality results. It is shown that the acceleration can be successfully applied and that the analysis of the results of different

*Corresponding author

acceleration approaches sheds some light on the physical meaning of the numerical approximations.

KEYWORDS: neutron transport, $P_N$ approximation, eigenvalue problem, Wynn-$\varepsilon$ acceleration techniques

## 1. INTRODUCTION

The determination of the eigenvalues of the neutron balance equation represents a significant problem in reactor physics. The mathematical problem can be given in different formulations, each one characterized by a specific physical interpretation. Some of these formulations are especially interesting to be studied: the multiplication or $k$-eigenvalue [1], the time or $\alpha$-eigenvalue [2], the effective multiplication factor per collision or $\gamma$ eigenvalue, originally introduced by Davison [3] and, finally, the effective density factor or $\delta$-eigenvalue, related to the overall atomic density of the system [4]. In a previous work [5] these formulations for the neutron transport eigenvalue equation have been studied, adopting a simplified geometrical 1D slab configuration, aiming at the analysis of the characteristics of the $P_N$ approach [6] to the numerical solution of these problems. Several benchmarks available in the literature have been used to compare the results obtained and some peculiar trends of convergence of the eigenvalue with respect to the order $N$ of the spherical harmonics approximation have been observed. In particular, the influence of the choice of the boundary conditions (Mark [7,8] or Marshak [9]) and the different patterns emerging when solved by odd-order and even-order $P_N$ have been detected.

In this contribution, we aim at focusing our attention on the convergence of the eigenvalue problem, referring to both the convergence of the single $P_N$ model, which is affected by spatial discretization errors, as well as the convergence to the "true" eigenvalue of the transport problem with increasing $N$. For this purpose, the possibility to apply acceleration techniques to the sequences of eigenvalues obtained in different problem setups are investigated. To perform this analysis we focus on the $k_{\text{eff}}$ formulation of the transport equation using the W-$\varepsilon$ acceleration scheme [10]. Results are compared to reference Monte Carlo values computed for this work.

## 2. THE WYNN-$\varepsilon$ ACCELERATION SCHEME

The Wynn-$\varepsilon$ acceleration [11] is but one algorithm of a wide class of accelerations called Shanks acceleration [12]. Accelerations find their use in calculus, which is limit-based. Essentially, all limit operations, convergent or not, lend themselves to numerical acceleration. An acceleration determines the asymptotic approach to the limit, usually reaching it more quickly than a simple consecutive approach of a sequence as a countable set. Accelerations are applicable to any sequence, convergent or not, in order to approximate the limit or anti-limit. Here, we consider only convergent sequences generated by solutions to the 1D transport equation in the spherical harmonics approximation and finite difference spatial discretization. The basic concept is to consider a finite sequence, say $n$, and determine a set of parameters assumed to represent the asymptotic behavior of the set as, in our case, the spherical harmonics order becomes large and the spatial discretization becomes small. In this way, one establishes a set of algebraic equations for the assumed parameters including an estimate of the limit. This final result amounts to a Padé approximant $(m, n)$. For the case $(n, n)$, Wynn very cleverly constructed the following algorithm and tableau:

$$\varepsilon_{-1}^{(m)} = 0, \tag{1}$$

$$\varepsilon_{0}^{(m)} = k_{\text{eff},m} \quad m = 0, \ldots, L, \tag{2}$$

$$\varepsilon_{k+1}^{(m)} = \varepsilon_{k-1}^{(m+1)} + \frac{1}{\varepsilon_k^{(m+1)} - \varepsilon_k^{(m)}} \qquad k = 0, \ldots, 2K-1; \;\; m = 0, \ldots, L, \tag{3}$$

where the sequence $k_{\text{eff},m}$ is to be accelerated to convergence. The resulting tableau is sketched in Figure 1. Then, every odd column becomes an approximation to the limit of the sequence, where the last entry is considered the "best" approximation (see arrow). Note that the sequence can have an irregular index, i.e. any stride. If we know all the terms of the sequence, then the tableau will grow on the fly as more terms of the sequence are included to hopefully provide a better approximation as $n$ increases.

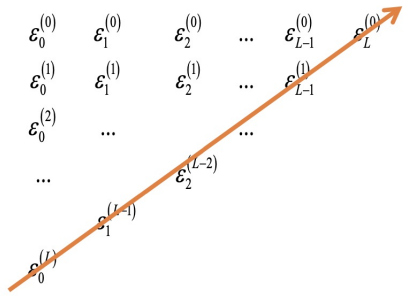


**Figure 1: Wynn tableau adopted to accelerate convergence.**

## 3. APPLICATION TO THE EIGENVALUE PROBLEM

Here we will apply W-$\varepsilon$ to find an optimized solution of the $P_N$ approximation to the 1D transport equation eigenvalue. Optimized, in our context, indicates a fully accelerated solution. We believe that our results will be the first instance of such a fully converged solution to the eigenvalue problem. It is recognized that for any numerical approximation using discretization and/or iteration, the solution will contain residual or truncation (discretization) errors, not to mention round-off errors. Convergence acceleration attempts to correct for these errors and can be thought of as a constructive sensitivity study with regard to error from a numerical method. Usually, one performs sensitivity studies to observe perturbations of a solution with respect to tightening or loosening of the imposed calculational error limits. They do not lead to a systematic correction, but to a general confirmation. Convergence acceleration, on the other hand, provides a systemic correction that could lead to an improved solution. Note that we characterize acceleration with words like "attempts" or "hopefully leads to" because, in practice, we are performing a numerical experiment. Like all experiments, we do not generally know the outcome, unless there is confirmatory theoretical data. Unfortunately, the theory of convergence acceleration does not include wide-reaching theory [13]. Thus, we can only observe and conjecture, exploiting, for the specific application, the results computed with the Monte Carlo method, which is usually assumed as a numerical reference within its statistical confidence interval.

Our experiment concerns a large number of $P_N$ solutions in the range $N$ = 1 through 1000 for one- and two-group characterizations of a critical Pu-239 slab reactor, whose physical data, taken from [14], where all eigenvalues are set to unity to five digits, are reported in Tables 1 and 2. Different $P_N$ eigenvalue sequences are generated according to the kind of boundary conditions (BCs) employed to approximate vacuum, i.e. Marshak and Mark boundary conditions. In the

| $\nu$ [-] | $\Sigma_t$ [cm$^{-1}$] | $\Sigma_f$ [cm$^{-1}$] | $\Sigma_{s,0}$ [cm$^{-1}$] | $\Sigma_{s,1}$ [cm$^{-1}$] | $\Sigma_{s,2}$ [cm$^{-1}$] |
|---|---|---|---|---|---|
| 2.5 | 1 | 0.266667 | 0.7333333 | 0.2 | 0.075 |

**Table 1: Material data for the one-group problem. The critical thickness is equal to 1.54064 cm.**

latter case, for even values of $N$, we distinguish between Mark A, i.e. the incoming directions for the vanishing flux are the roots of the Legendre polynomial $P_{N+1}$ excluding 0, and Mark B, when the roots of $P_N$ are employed.

| $\nu_1$ [-] | $\Sigma_1$ [cm$^{-1}$] | $\Sigma_{f,1}$ [cm$^{-1}$] | $\Sigma_{1\to1}$ [cm$^{-1}$] | $\Sigma_{1\to2}$ [cm$^{-1}$] | $\chi_1$ [-] |
|---|---|---|---|---|---|
| 3.1 | 0.22080 | 0.09360 | 0.07920 | 0.04320 | 0.575 |
| $\nu_2$ [-] | $\Sigma_2$ [cm$^{-1}$] | $\Sigma_{f,2}$ [cm$^{-1}$] | $\Sigma_{2\to1}$ [cm$^{-1}$] | $\Sigma_{2\to2}$ [cm$^{-1}$] | $\chi_2$ [-] |
| 2.93 | 0.33600 | 0.08544 | 0 | 0.23616 | 0.425 |

**Table 2: Material data for the two-group problem. The critical thickness is equal to 3.5912040 cm.**

We perform convergence acceleration on both the spherical harmonics order and the spatial discretization to achieve a truly, fully converged transport solution. Converging both sequences is a novel application of the algorithm. W-$\varepsilon$ acceleration allows a window to span every, say, 15 elements of the sequence for example, where only the elements in the window are accelerated. The window advances through the sequence one term at a time. This strategy assumes that the early terms of the sequence are less precise than the later terms so they should be given less importance than the following ones. Overall spherical harmonics and spatial convergence comes by performing spatial convergence for each set of $P_N$ approximations at finer and finer spatial discretizations. The W-$\varepsilon$ action is to converge the $P_N$ approximations at each spatial discretization and then converge the spatial discretizations across $P_N$ approximations. There are many ways to make sequences and we believe that this is the most intuitive and straightforward.

## 4. RESULTS

Figures 2 to 4 display, on the left, the relative errors between two consecutive $k_{\text{eff}}$'s of the unaccelerated solution (solid line) and for the accelerated sequence (colored dots) for each of four of seven discretizations employed ($N_x$=10, 20, 40, 80, 160, 320, 640 spatial points), while the ratio of the relative errors of the unaccelerated to the accelerated eigenvalues is shown on the right, considering the different boundary condition options. It should be noted that, if the ratio is greater than unity, the precision advantage goes to acceleration. This is the first of two examples of accelerations (one and two groups). It is obvious that the W-$\varepsilon$ acceleration generally gives a more precise $k_{\text{eff}}$ by several orders of magnitude. From these figures, it is quite evident that W-$\varepsilon$ can provide up to seven orders of acceleration, although there are several dozen of points where the unaccelerated is more precise, mostly occurring for low $N$. It can be noticed by inspection that, after a strong error decay at low $N$, the points become more scattered for increasing spherical harmonics orders, which is

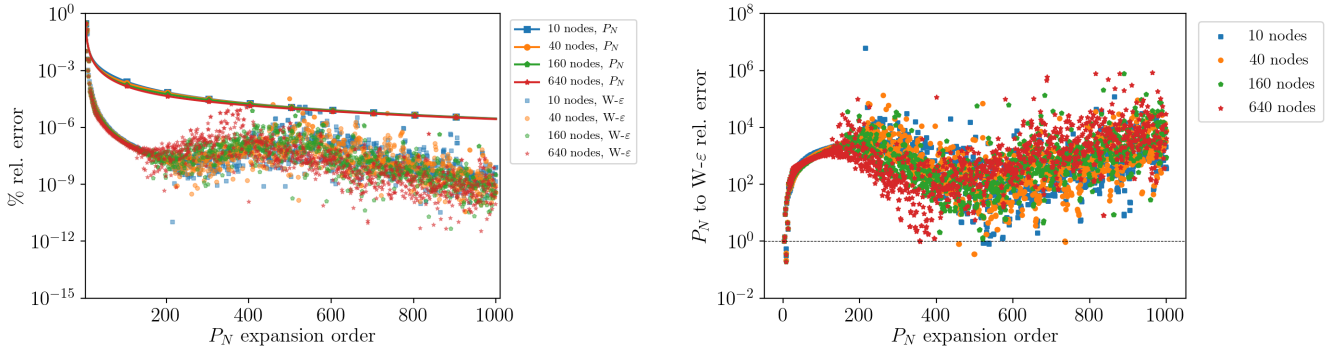


**Figure 2: Relative difference between two successive iterates for the original and accelerated sequences (left) and original to accelerated sequences ratio using Mark A BCs for a two-group critical Pu-239 slab.**

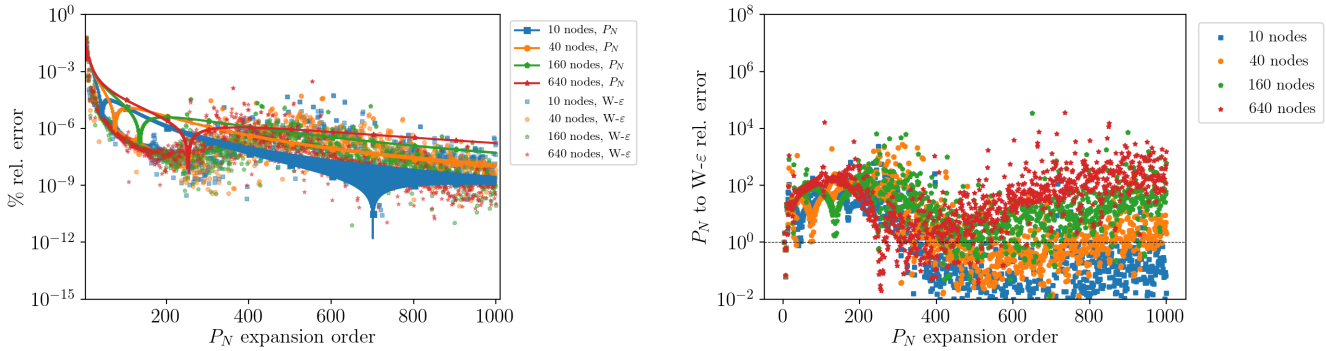


**Figure 3: Relative difference between two successive iterates for the original and accelerated sequences (left) and original to accelerated sequences ratio using Mark B BCs for a two-group critical Pu-239 slab.**

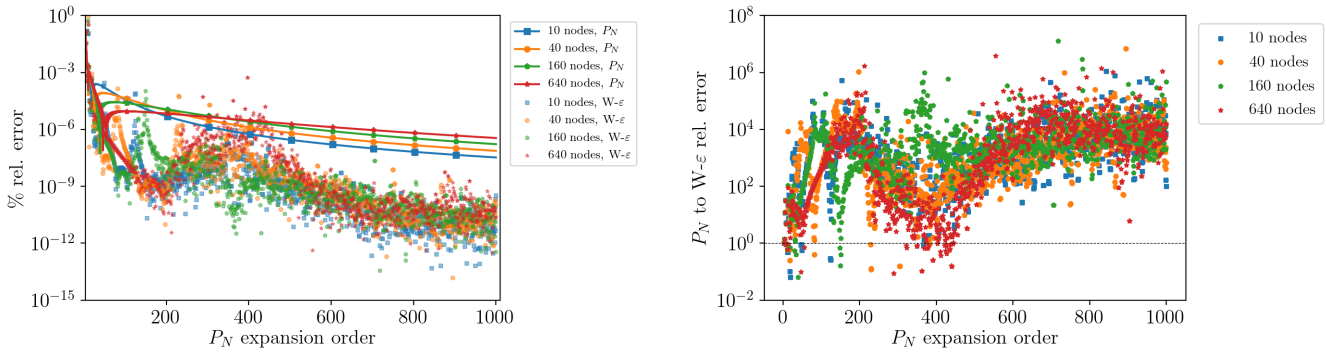


**Figure 4: Relative difference between two successive iterates for the original and accelerated sequences (left) and original to accelerated sequences ratio using Marshak BCs for a two-group critical Pu-239 slab.**

likely due to the truncation error. It is interesting to observe that, when Mark B BCs are imposed, the relative errors of the original sequences for the cases with 10 and 20 nodes show an oscillat-

ing behaviour, which is likely to be the cause for the reduced acceleration. These oscillations are damped when finer spatial discretizations are employed. In such a case, the relative difference between the accelerated sequence becomes better than the original sequence one, as clearly visible in Figure 3 on the right.

| $N_x$ | No W-$\varepsilon$ | W-$\varepsilon$ ($N$) | W-$\varepsilon$ ($N_x$) | W-$\varepsilon$ ($N$, $N_x$) |
|---|---|---|---|---|
| 10 | 0.99813885 | 0.99813705 | 0.99813885 | 0.99813705 |
| 20 | 0.99947502 | 0.99947326 | 0.99947502 | 0.99947326 |
| 40 | 0.99984927 | 0.99984754 | 0.99999488 | 0.99999318 |
| 80 | 0.99995775 | 0.99995608 | 1.00000203 | 1.00000040 |
| 160 | 0.99998917 | 0.99998765 | 1.00000198 | 1.00000060 |
| 320 | 0.99999800 | 0.99999674 | 1.00000203 | 1.00000050 |
| 640 | 1.00000036 | 0.99999933 | 1.00000108 | 1.00000034 |
| Monte Carlo | | $1.000000344 \pm 3.401 \cdot 10^{-6}$ | | |

**Table 3: Unaccelerated and accelerated sequences for the two-group problem, obtained with $N$=1000 imposing Mark A BCs. The Monte Carlo result is provided with a confidence interval of 2$\sigma$.**

| $N_x$ | No W-$\varepsilon$ | W-$\varepsilon$ ($N$) | W-$\varepsilon$ ($N_x$) | W-$\varepsilon$ ($N$, $N_x$) |
|---|---|---|---|---|
| 10 | 0.998136907 | 0.998136886 | 0.998136907 | 0.998136886 |
| 20 | 0.999473142 | 0.999473096 | 0.999473142 | 0.999473096 |
| 40 | 0.999847491 | 0.999847387 | 0.999993182 | 0.999993027 |
| 80 | 0.999956149 | 0.999955928 | 1.00000059 | 1.00000026 |
| 160 | 0.999987812 | 0.999987487 | 1.00000084 | 1.00000043 |
| 320 | 0.999996815 | 0.999996636 | 1.00000067 | 1.00000038 |
| 640 | 0.999999235 | 0.999999203 | 0.999999905 | 1.00000046 |
| Monte Carlo | | $1.000000344 \pm 3.401 \cdot 10^{-6}$ | | |

**Table 4: Unaccelerated and accelerated sequences for the two-group problem, obtained with $N$=1000 imposing Marshak BCs. The Monte Carlo result is provided with a confidence interval of 2$\sigma$.**

The final step is to accelerate across the spatial discretizations. In Tables 3 and 4, we see the true power of W-$\varepsilon$ acceleration. The first two columns (identified by No W-$\varepsilon$ and W-$\varepsilon$ ($N$)) are the last $k_{\text{eff}}$'s from Figure 2 at $N$=1000 for each discretization identified by the number of spatial points $N_x$. These values should be the most converged for the unaccelerated and accelerated sequences. The last two columns (identified by W-$\varepsilon$ ($N_x$) and W-$\varepsilon$ ($N$, $N_x$)) are the W-$\varepsilon$ accelerations of the first two columns across discretization. The results are quite informative. The spherical harmonics accelerated values are very similar at each discretization, but approach unity with finer discretizations, as anticipated. When columns 1 and 2 are accelerated in discretization, the values become even closer to unity and eventually overtake unity at the 1/100 of pcm level. When compared with Monte Carlo results, we observe an excellent agreement up to $2 \cdot 10^{-2}$ pcm. The agreement is even

more remarkable when one considers that in all the $P_N$ solutions there are only 14 values out of 7000 that are above 1. So, it seems, W-$\varepsilon$ is truly finding the $k_{\text{eff}}$.

To show that this excellent agreement is real and not a fluke, we consider the one-group case. Figures 5 to 7 show the same plots as for the two-group case indicating the same degree of acceleration. Table 5 shows the acceleration across the dicretizations. However, full agreement to the seventh digit on rounding comes when acceleration is applied to the spatial discretizations. The agreement is simply outstanding.

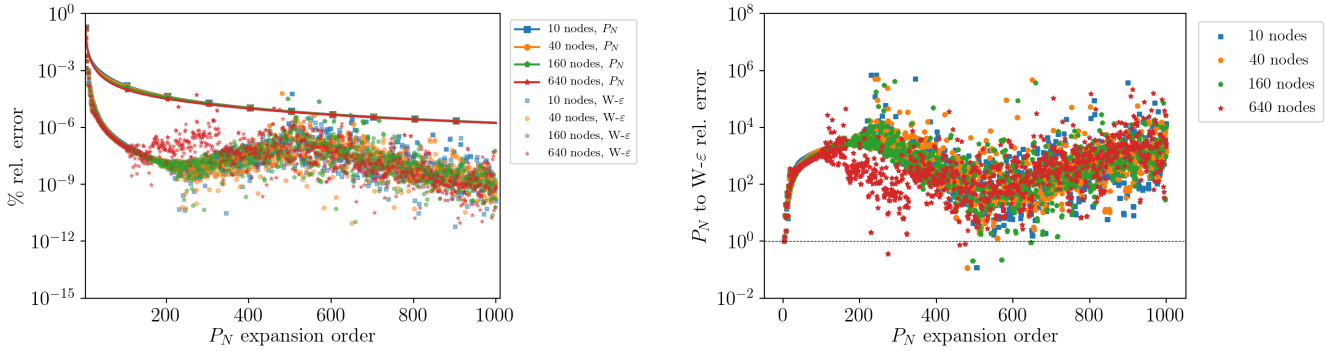


**Figure 5: Relative difference between two successive iterates for the original and accelerated sequences (left) and original to accelerated sequences ratio using Mark A BCs for a one-group critical Pu-239 slab.**

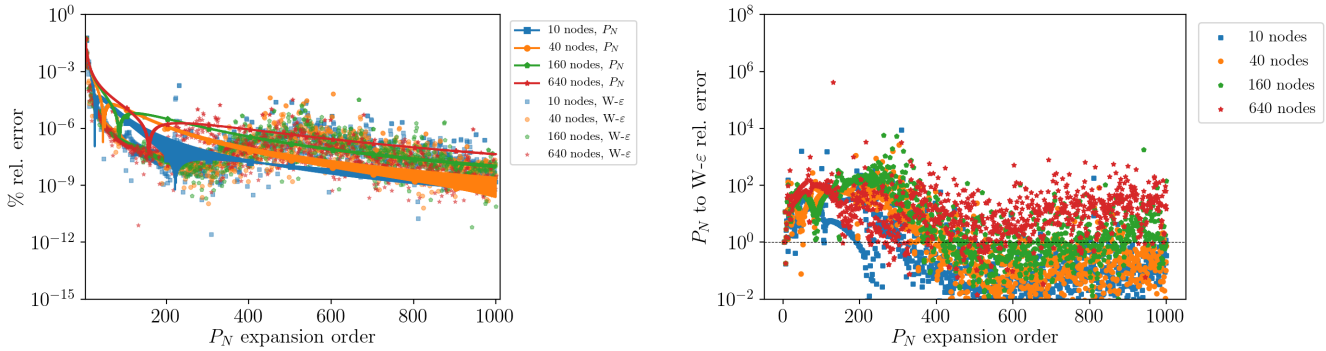


**Figure 6: Relative difference between two successive iterates for the original and accelerated sequences (left) and original to accelerated sequences ratio using Mark B BCs for a one-group critical Pu-239 slab.**

Figure 8 shows the effectiveness of the W-$\varepsilon$ acceleration scheme with respect to the Monte Carlo reference for the one- and two-group cases. All the eigenvalues fall within the $2\sigma$ confidence interval, represented by the shaded area, with some important differences. The first group of values on the left is the best $P_N$ estimate, with $N = 1000$ and $N_x = 640$, while the second group shows the spherical harmonics accelerated results for the same number of meshes. It is interesting to notice that the spherical harmonics acceleration shrinks the differences due to the boundary conditions, but leaves some bias with respect to the Monte Carlo result due to the inaccurate treatment of the spatial variable. Similarly, when the spatial acceleration is performed on the $N = 1000$ case, the

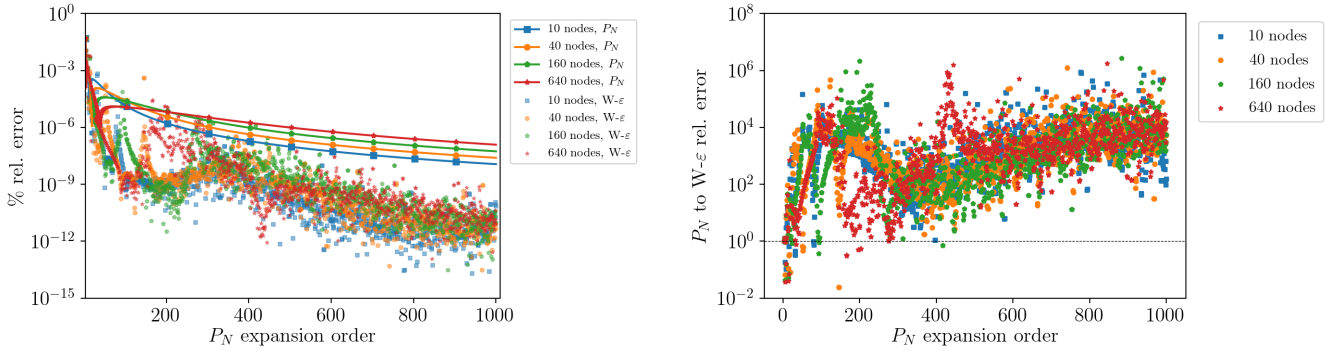


**Figure 7: Relative difference between two successive iterates for the original and accelerated sequences (left) and original to accelerated sequences ratio using Marshak BCs for a one-group critical Pu-239 slab.**

| $N_x$ | No W-$\varepsilon$ | W-$\varepsilon$ ($N$) | W-$\varepsilon$ ($N_x$) | W-$\varepsilon$ ($N$, $N_x$) |
|---|---|---|---|---|
| 10 | 0.99783010 | 0.99782900 | 0.99783010 | 0.99782900 |
| 20 | 0.99937445 | 0.99937338 | 0.99937445 | 0.99937338 |
| 40 | 0.99982891 | 0.99982786 | 1.00001840 | 1.00001737 |
| 80 | 0.99996565 | 0.99996462 | 1.00002451 | 1.00002349 |
| 160 | 1.00000653 | 1.00000554 | 1.00002401 | 1.00002305 |
| 320 | 1.00001848 | 1.00001760 | 1.00004181 | 1.00002137 |
| 640 | 1.00002180 | 1.00002112 | 1.00002257 | 1.00002257 |
| Monte Carlo | | $1.000022654 \pm 3.376 \cdot 10^{-6}$ | | |

**Table 5: Unaccelerated and accelerated sequences for the one-group problem, obtained with N=1000 imposing Mark A BCs. The Monte Carlo result is provided with a confidence interval of $2\sigma$.**

algorithm provides an extrapolation with respect to space but does not provide an improvement in the transport phenomena detail. However, when the full Wynn-$\varepsilon$ acceleration is applied, all the eigenvalues cluster around the Monte Carlo reference. This practical evidence can be observed also for larger values of $N$, as shown in Figure 9, where a more limited sequence of values is used, in the range $N$=1980 through 2000, which saves significant computational time.

## 5. CONCLUSIONS

In this work the W-$\varepsilon$ acceleration approach is applied to improve the estimate of the $k_{\text{eff}}$ eigenvalue using the $P_N$ approximation for the neutron transport equation in plane geometry within one- and two-group models. It is shown that the acceleration scheme is highly effective and provides accurate results as compared to Monte Carlo, used as a reference. This paper demonstrates, for the first time, the concept of a true deterministic transport solution defined as a solution fully converged in all discrete approximations.

In a future work, the same technique will be applied to different formulations of the eigenvalues, to the estimation of higher-order eigenvalues and perhaps non-critical configurations. The study

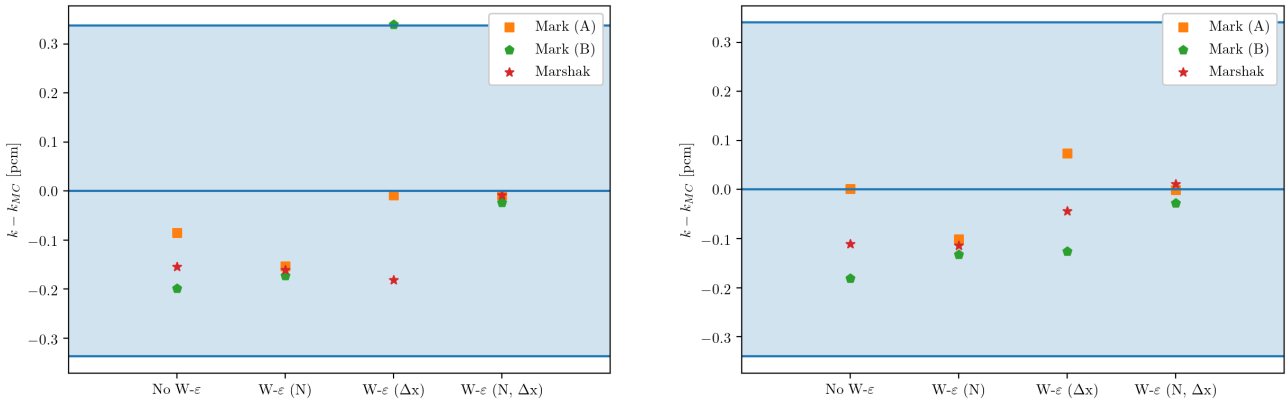


**Figure 8: Differences between $P_N$ $k_{\text{eff}}$ values and the Monte Carlo reference for the one- (left) and two-group (right) critical Pu-239 slab problems. The angular expansion order ranges from 1 to 1000.**

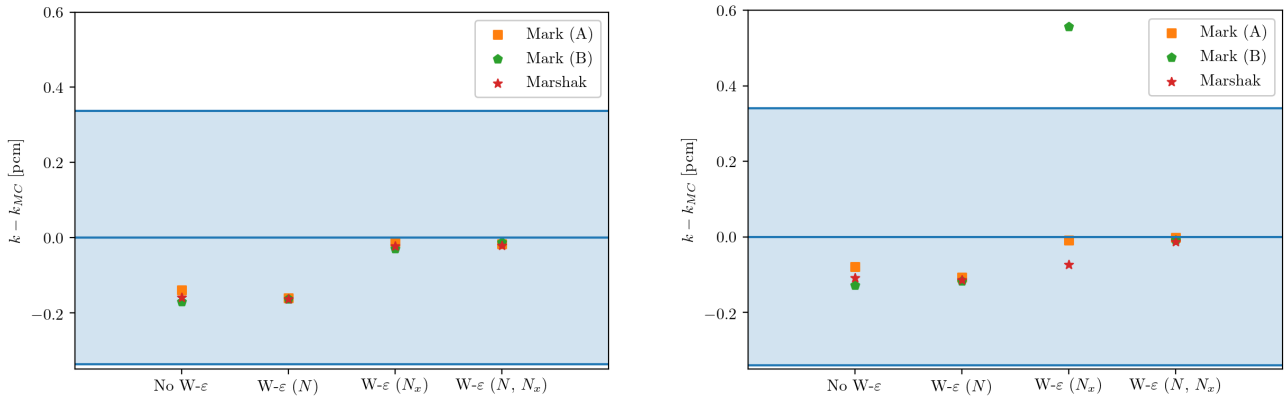


**Figure 9: Differences between $P_N$ $k_{\text{eff}}$ values and the Monte Carlo reference for the one- (left) and two-group (right) critical Pu-239 slab problems. The angular expansion order ranges from 1980 to 2000.**

will be also extended to investigate the possibility to apply the acceleration for the estimation of the eigenfunctions. Finally, this technique begs for the application of parallel processing. The application of convergence acceleration demonstrated here is called ex-code convergence. Ex-code refers to the determination of the entire sequence before hand and then applying W-$\varepsilon$ for convergence. This is in contrast to in-code convergence, where the W-$\varepsilon$ tableau is constructed on-the-fly and likewise compared to the original sequence error. Thus, a code's precision is rendered on the fly saving significant computation time, especially in light of parallel computing.

## REFERENCES


[1] G. Bell and S. Glasstone. *Nuclear Reactor Theory*. Van Nostrand Reinhold (1970).

[2] A. Zoia, E. Brun, and F. Malvagi. "Alpha eigenvalue calculations with TRIPOLI-4®." *Annals of Nuclear Energy*, **volume 63**, pp. 276 – 284 (2014).

[3] B. Davison. *Neutron Transport Theory*. University Press, Oxford (1958).

[4] D. G. Cacuci, Y. Ronen, Z. Shayer, J. J. Wagschal, and Y. Yeivin. "Eigenvalue-dependent neutron energy spectra: definitions, analyses, and applications." *Nuclear Science and Engineering*, **volume 81**, pp. 432–442 (1982).

[5] N. Abrate, M. Burrone, S. Dulla, P. Ravetto, and P. Saracco. "Eigenvalue Formulations for the $P_N$ Approximation to the Neutron Transport equation." *Journal of Computational and Theoretical Transport*, **volume 49**, pp. 1–23 (2020).

[6] R. V. Meghreblian and D. K. Holmes. *Reactor Analysis*. McGraw-Hill, New York (1960).

[7] J. Mark. "The spherical harmonics method, Part I, Atomic Energy Report 92, National Research Council of Canada." (1944).

[8] J. Mark. "The spherical harmonics method, Part II, Atomic Energy Report 97, National Research Council of Canada." (1945).

[9] R. Marshak. "Note on the spherical harmonics method as applied to the Milne problem for a sphere." *Physical Review*, **volume 71**, pp. 443–446 (1947).

[10] B. Ganapol. "More Than You Wanted to Know About Convergence Acceleration." In *Radiation Protection and Shielding Division Workshop (ANS), Knoxville, TN* (2014).

[11] P. Wynn. "On a device for computing the em(Sn) transformation." *Math Tables Aids Comput*, **volume 10**, pp. 91–96 (1956).

[12] D. Shanks. "Nonlinear Transformations of Divergent and Slowly Convergent Sequences." *J Math Phys*, **volume 34**, pp. 1–42 (1955).

[13] A. Sidi. *Practical Extrapolation Methods*. Cambridge University Press (2003).

[14] A. Sood, R. A. Forster, and D. K. Parsons. "Analytical benchmark test set for criticality code verification." *Progress in Nuclear Energy*, **volume 42**, pp. 55–106 (2003).